OPEN ACCESS Freely available online

PLoS one

K_V7/KCNQ Channels Are Functionally Expressed in Oligodendrocyte Progenitor Cells

Wei Wang[•], **Xiao-Fei Gao**[•], **Lin Xiao, Zheng-Hua Xiang, Cheng He***

Institute of Neuroscience and Key Laboratory of Molecular Neurobiology of the Ministry of Education, Neuroscience Research Center of Changzheng Hospital, Second Military Medical University, Shanghai, China

Abstract

Background: K_V7/KCNQ channels are widely expressed in neurons and they have multiple important functions, including control of excitability, spike afterpotentials, adaptation, and theta resonance. Mutations in KCNQ genes have been demonstrated to associate with human neurological pathologies. However, little is known about whether K_V7/KCNQ channels are expressed in oligodendrocyte lineage cells (OLCs) and what their functions in OLCs.

Methods and Findings: In this study, we characterized K_V7/KCNQ channels expression in rat primary cultured OLCs by RT-PCR, immunostaining and electrophysiology. KCNQ2-5 mRNAs existed in all three developmental stages of rat primary cultured OLCs. K_V7/KCNQ proteins were also detected in oligodendrocyte progenitor cells (OPCs, early developmental stages of OLCs) of rat primary cultures and cortex slices. Voltage-clamp recording revealed that the I_M antagonist XE991 significantly reduced K_V7/KCNQ channel current ($I_{K(Q)}$) in OPCs but not in differentiated oligodendrocytes. In addition, inhibition of K_V7/KCNQ channels promoted OPCs motility in vitro.

Conclusions: These findings showed that K_V7/KCNQ channels were functionally expressed in rat primary cultured OLCs and might play an important role in OPCs functioning in physiological or pathological conditions.

Citation: Wang W, Gao X-F, Xiao L, Xiang Z-H, He C (2011) K_V7/KCNQ Channels Are Functionally Expressed in Oligodendrocyte Progenitor Cells. PLoS ONE 6(7): e21792. doi:10.1371/journal.pone.0021792

Editor: Ya-Ping Tang, Louisiana State University Health Sciences Center, United States of America

Received October 12, 2010; **Accepted** June 12, 2011; **Published** July 5, 2011

Funding: National Natural Science Foundation (30800430), National Key Basic Research Program (2007CB947100, 2011CB504401), and the Ministry of Science and Technology of China (2009ZX09311-001). The funders had no role in study design, date collection and analysis, decision to publish, or preparation of the manuscript.

Competing Interests: The authors have declared that no competing interests exist.

* E-mail: chenghe@smmu.edu.cn

• These authors contributed equally to this work.

Introduction

The KCNQ gene family encodes five voltage-gated delayed rectifier K^+ channels K_V7.1-5, and four of these K_V7.2-5 are expressed in the nervous system [1,2]. There they form subunits of voltage-gated K^+ channel originally termed the 'M-channel' and the current called M current, which has been demonstrated to assist in stabilizing the membrane potential in the presence of depolarizing currents and contributing to the resting potential of neurons [3,4]. In CNS, K_V7 channels form through homo- or heteromeric assembly of K_V7.2 to K_V7.5 subunits. So far, homomeric compositions are shown for K_V7.2-5 subunits; heteromeric compositions are represented by K_V7.2+3, K_V7.3+4 and K_V7.3+5 channels [2]. In most neurons native K_V7 channels are composed of K_V7.2 and K_V7.3 subunits [5] or sometimes of homomeric K_V7.2 subunits [6,7], although probably with a contribution by K_V7.5 subunits in some neurons [8]; K_V7.4 subunits are predominantly expressed in the auditory and vestibular systems, but also probably contribute to K_V7 channels in central dopaminergic neurons [9]. Recent evidences suggest that K_V7 channels have profound effects on neuronal excitability [10–15]. Inhibition of channel activity, by either a blocking drug such as linopirdine (DuP 996) [16] or 10, 10-bis(4-pyridinyl- methyl)-9(10 H)-anthracenone (XE991), or expression of a dominant-negative K_V7.2 construct, strongly enhances repetitive firing and even effects postnatal brain development [17]. Their mutations have been associated with human neurological pathologies including auditory diseases [1,2]. Mutations in either K_V7.2 or K_V7.3 lead to benign familial neonatal seizures [18] as do mutations in K_V7.5 [19,20]. In addition, mutations in K_V7.4 are associated with progressive hearing loss [21–23].

Oligodendrocytes are generated from oligodendroglial progenitor cells (OPCs) which proliferate in the subventricular zone and migrate to formative white matter regions, where they further proliferate, differentiate, and form myelin sheaths around axons [24,25]. Migration of OPCs is an essential step not only during the early stage of oligodendrocyte lineage cells (OLCs) development but also in some demyelination pathological conditions such as Multiple Sclerosis (MS) and other variety of CNS injuries [26–28]. Several ion channels have been identified recently in OLCs to participate in regulation of OPCs migration including K_V 3.1[29], voltage gated Ca^{2+} channel [30,31] P2X7 receptor [32], GABA receptor [33], glutamate (AMPA and/or kainate) receptor [34] etc. In addition, previous studies indicated that the various K^+ channels were linked to cell migration. Kv7.1 has been reported to regulate invasiveness of stem-like cell types [35]. Activation of K_V channel promotes migration of intestinal

epithelial cells [36]. $K_V10.1$ is involved in adhesion and viability of CHO cells [37]. $K_V11.1$ participates in tumor cells invasion [38] and inhibition of $K_V1.3$ suppresses the motility and activation of effector memory T (Tem) cells [39]. OLCs express all six members of the delayed rectifier Shaker family K^+ channels, Kv1.1–Kv1.6 [40–45], inwardly rectifying K^+ (K_{ir}) channels Kir2.1, Kir1.1 and Kir4.1 [46,47] and Kv3.1[29]. However, whether OLCs functionally express K_V7 channels is still unknown. In this paper, we studied the expression and function of K_V7 channels in OLCs.

Results

The mRNAs of $K_V7.2$–5/ KCNQ2-5 were detected in rat primary cultured OLCs

Immunocytochemical markers allow for the distinction of three consecutive phenotypically defined stages of OLCs development in vitro: the bipolar $GFAP^-A2B5^+NG2^+$ OPCs, multipolar $O4^+GalC^-$ IOs, and complex process bearing MBP^+GalC^+ MOs [48,49]. In the present study, we got highly pure $GFAP^-A2B5^+NG2^+$ OPC cultures (98.8±0.2%, assessed by immunocytochemical staining) (Fig.1 A, B). In differentiation medium, OPCs developed into $O4^+$ IOs and MBP^+ MOs (Fig.1 C, D). As KCNQ1 was not detected in neural system [1,2], we examined the mRNAs of KCNQ2-5 in cultured OLCs by RT-PCR. We found that KCNQ2-5 mRNA were all present in cultured OPCs (Fig.2A left). KCNQ5 was undetectable in IOs (Fig.2C left). In MOs, only KCNQ4 was detectable very weakly (Fig.2D left). No positive line was present in negative control which implied that the mRNA was not contaminated with genome DNA (Fig.2A, C, D right).

Localization of $K_V7.2$-5/ KCNQ2-5 in OLCs

The expression of $K_V7.2$-5 in cultured OLCs was further confirmed by immunostaining. The antibodies of anti-NG2, anti-O4 and anti-MBP were used to identify OPCs, IOs, and MOs in cultures respectively. The staining for $K_V7.2$-5 was on the soma and processes of OPCs. The immunofluorescence signals were positive in both the cytoplasm and the cell membrane of OPCs (Fig.3A–D). With the maturation of OLCs, the immunofluorescence signals of $K_V7.2$-5 became weaker and were restricted to the cell bodies in IOs, and MOs. (Fig.3E–H, I–L). Immunohistochemistry was also performed to verify the expression of $K_V7.2$-5 proteins in OPCs in vivo. In cortex, $K_V7.2$, 3 or 5 were detected to localize on a part of $NG2^+$ OPCs (26±9%, 27.1±11% and 30.5±7% respectively) (Fig.4A–C, a1–a3; d1–d3; g1–g3), while other part of $NG2^+$ OPCs did not express $K_V7.2$, 3 or 5 (Fig.4A–C, b1–b3; e1–e3; h1–h3). We also found that some cells, which expressed $K_V7.2$, 3 or 5, were not NG2 positive (Fig.4A–C, c1–c3; f1–f3; i1–i3). Those cells may be neurons or other glia cells. All $NG2^+$ cells were $K_V7.4$ negative (Fig.4D, j1–j3).

K_V7/KCNQ Channel currents ($I_{K(Q)}$) in OLCs

In order to determine the K_V7 channels are functionally expressed in OLCs, we recorded 61 cultured OLCs with whole-cell patch clamp recording to evaluate the electrophysiological property of the currents. In an attempt to isolate the K_V7 channel currents from other voltage-gated K^+ currents, the membrane potential was held at a relatively depolarized potential (−20 mV) to activate K_V7 channels [3,50] and to inactivate many of the other K^+ channels that activate in this membrane potential region [51–53]. The membrane potential was then stepped down to more hyperpolarized potentials (−60 mV, in 10 mV decrements) for

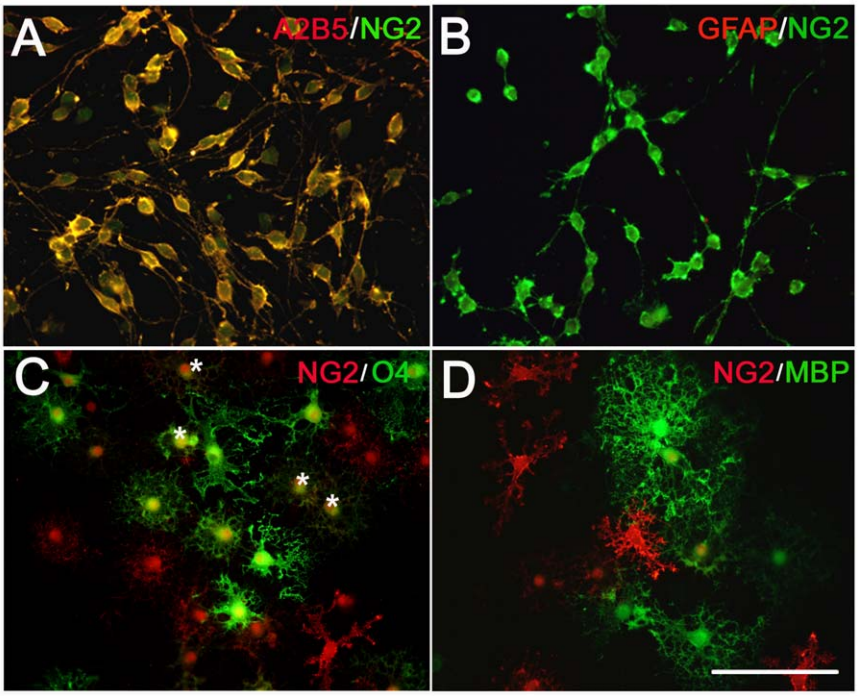

Figure 1. Morphological and immunostaining characterization of OLCs in rat primary cultures. (A) Double immunostaining of cultured OPCs showing that A2B5-positive cells (red) were also immunopositive for anti-NG2 (green). (B) OPCs (NG2-positive, green) were negative for anti-GFAP (red). (C) There were NG2-positive cells (red) after differentiation in T3 contained medium for two days. Immature oligodendrocytes (IOs) were stained with O4 antibody (green), a marker of IOs. Some cells co-localized with O4 and NG2 (Asterisk) (D) Four days later, NG2-positive cells (red) still existed and mature oligodendrocytes (MOs) were stained with MBP antibody (green), a marker of MOs. Scar bar = 100 μm.
doi:10.1371/journal.pone.0021792.g001

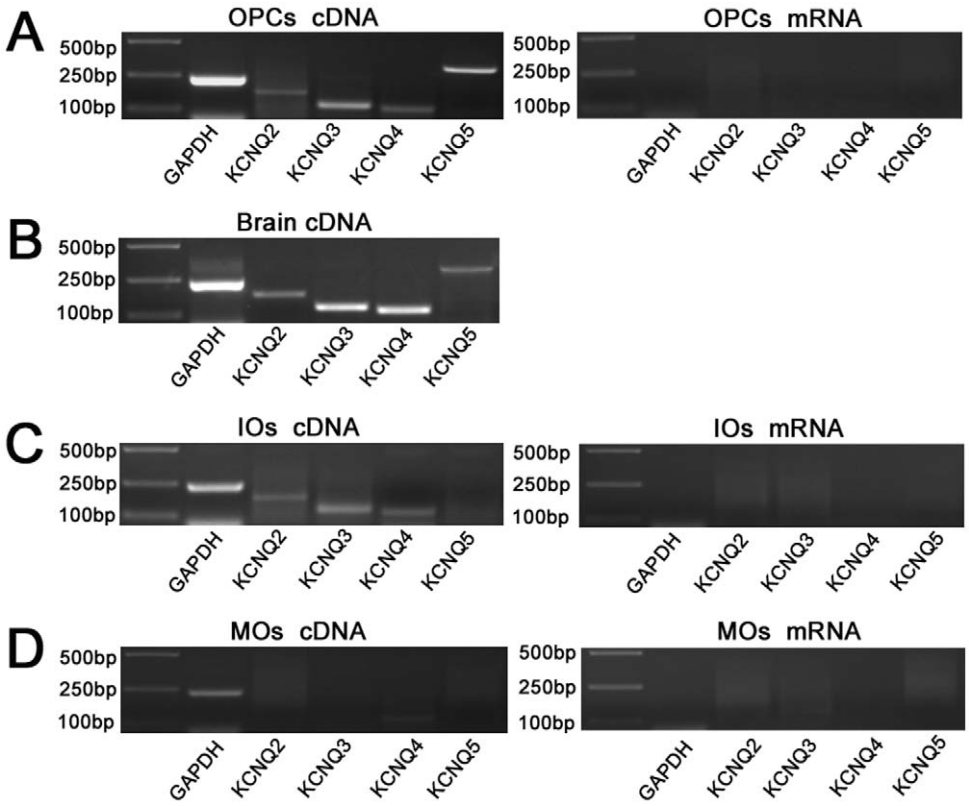

Figure 2. RT-PCR analysis for primary cultured OLCs. (A–D, left) The mRNA of GAPDH (243 bp), KCNQ2 (172 bp), KCNQ3 (121 bp), KCNQ4 (110 bp) and KCNQ5 (320 bp) was identified in OLCs and whole forebrain (positive control) by RT-PCR. (A, C, D, right) RNA from OLCs without reverse transcription was performed PCR procedure directly as negative control.
doi:10.1371/journal.pone.0021792.g002

1 s to deactivate the K_V7 channels (Fig.5A). The amplitude of the $I_{K(Q)}$ was measured as the difference between the instantaneous current at the onset of hyperpolarization and the steady-state current at the end of voltage command [3] (Fig.5A, right). Fig.5B shows the current–voltage relationship of $I_{K(Q)}$ from 17 OPCs. The mean $I_{K(Q)}$ amplitude was voltage dependent and the maximal $I_{K(Q)}$ amplitude (61.16±6.32 pA) was measured at −40 mV. The deactivation time constant of $I_{K(Q)}$ was determined by fitting the current curves measured at each voltage with a single exponential function. Fig.5C shows the mean deactivation time constant of $I_{K(Q)}$ as a function of voltage (n = 17). The mean $I_{K(Q)}$ deactivation time constant was 292.94±26.79 ms (−30 mV), 246.94±24.97 ms (−40 mV), 152.85±17.59 ms (−50 mV) and 131.89±14.18 ms (−60 mV), indicating that it was voltage dependent. Note that the deactivation time constant was a linear function of voltage (correlation coefficient r = 0.93) and was shorter at more negative membrane potentials which means at these potentials, $I_{K(Q)}$ was deactivated faster. We also recorded $I_{K(Q)}$ in IOs and MOs and the inward deactivation relaxation currents were almost not existed. (Fig.6C, D). Consequently, in this study, the characterizations of $I_{K(Q)}$ mainly were obtained from OPCs.

XE991 has been shown to be a potent and selective inhibitor for M current (I_M) in native neurons and currents from artificial expressed K_V7 channels [5] and has little impact on Kv2.1 [54]. In our experiments, $I_{K(Q)}$ was monitored with a 1-s-long hyperpolarizing voltage stepped from a holding potential of −20 to −40 mV. XE991 (10 μM) reduced about 46.1±6.8% $I_{K(Q)}$ in OPCs. Higher concentration of XE991 (30 μM) inhibited $I_{K(Q)}$ more than a half (by 67.4±5.6%) (Fig.6 A, B). Fig.6E shows the pooled concentration–response curve which plots the mean percentage inhibition of $I_{K(Q)}$ amplitude versus the log concentration of XE991 from 54 OPCs. The mean inhibition of $I_{K(Q)}$ by XE991 was 19.5±3.1% (at 1 μM), 33.3±5.7% (at 3 μM) and 80.1±4.2% (at 100 μM). The mean data was fitted with the Hill equation (see METHODS). The IC50 for XE991 was 13.3 μM and the power term n (Hill slope), which is related to the steepness of curve was 0.63. The goodness of fit R^2 was 0.99. In contrast, the currents in IOs and MOs were very insensitive to XE991 (Fig.6 C, D).

Previous studies reported that different K_V7 channel proteins have different sensitivities to TEA [55;56;5], and therefore it was of interest to examine the TEA sensitivity of $I_{K(Q)}$ in OPCs. The voltage protocol used to measure $I_{K(Q)}$ is the same as XE991 on $I_{K(Q)}$ recorded in OLCs. We then applied TEA at concentrations ranging from 0.3 mM to 30 mM. TEA caused a concentration dependent reduction in $I_{K(Q)}$ in OPCs. Fig.6F shows the pooled concentration–response curve which plots the mean percentage inhibition of $I_{K(Q)}$ amplitude versus the log concentration of TEA from 20 OPCs. The mean inhibition of $I_{K(Q)}$ by TEA was 33.3%±5.1% (0.3 mM), 54.7%±2.4% (1 mM), 72.1%±5.5% (3 mM), 87%±4.6% (10 mM) and 92.8%±1.2% (30 mM). Application of 30 mM TEA completely abolished the current. The mean data was fitted with the Hill equation (see METHODS). The IC50 for TEA was 0.84 mM and the power term n (Hill slope) was 0.7. The goodness of fit R^2 was 0.99.

The inhibition of K_V7/KCNQ channels promotes OPCs motility in *vitro*

Besides the electrophysiological properties of the K_V7 channels, we also investigated the effect of these channels on OPCs migration, which is important for myelin development. We

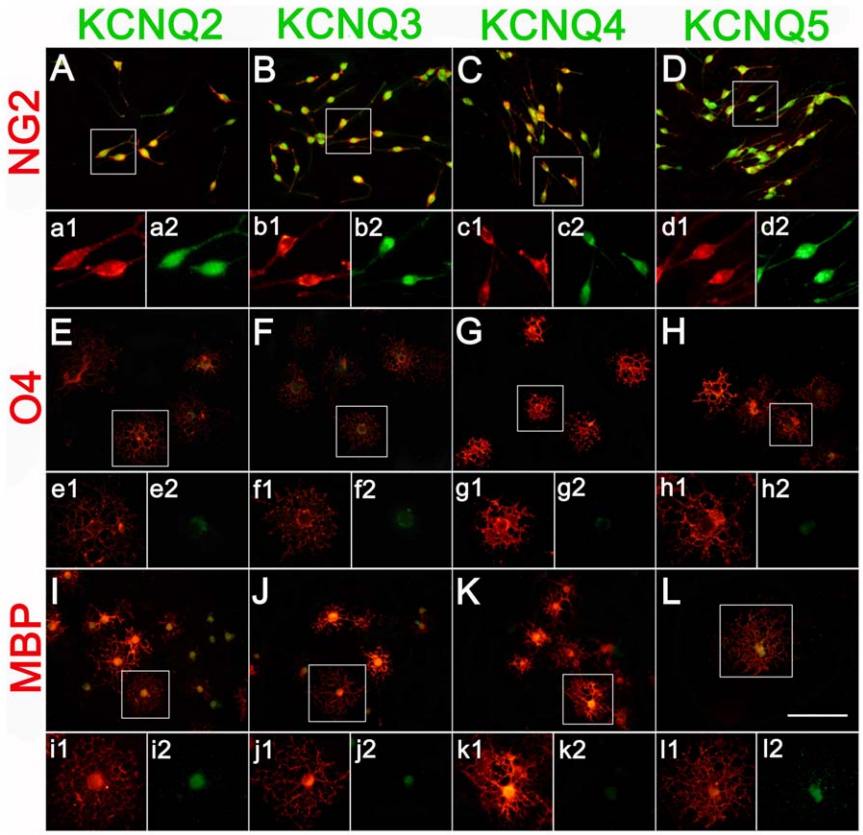

Figure 3. Immunofluorescence localization of K_V7.2-5/KCNQ2-5 subunits on the OLCs in rat primary cultures. (A–D) Co-localization of immunostaining for K_V7.2-5 subunits (green) and OPCs (NG2-positive, red) is displayed in the merged image. Higher magnification of the boxed area in A, B, C, D was shown in a1, a2; b1,b2; c1,c2; d1,d2. (E–H) The expression of K_V7.2-5 subunits (green) on IOs (O4-positive, red). Higher magnification of the boxed area in E, F, G, H was shown in e1, e2; f1,f2; g1,g2; h1,h2. (I–L) The expression of K_V7.2-5 subunits (green) on MOs (MBP-positive, red). Higher magnification of the boxed area in I, J, K, L was shown in i1, i2; j1,j2; k1,k2; l1,l2. Scar bar = 100 μm.
doi:10.1371/journal.pone.0021792.g003

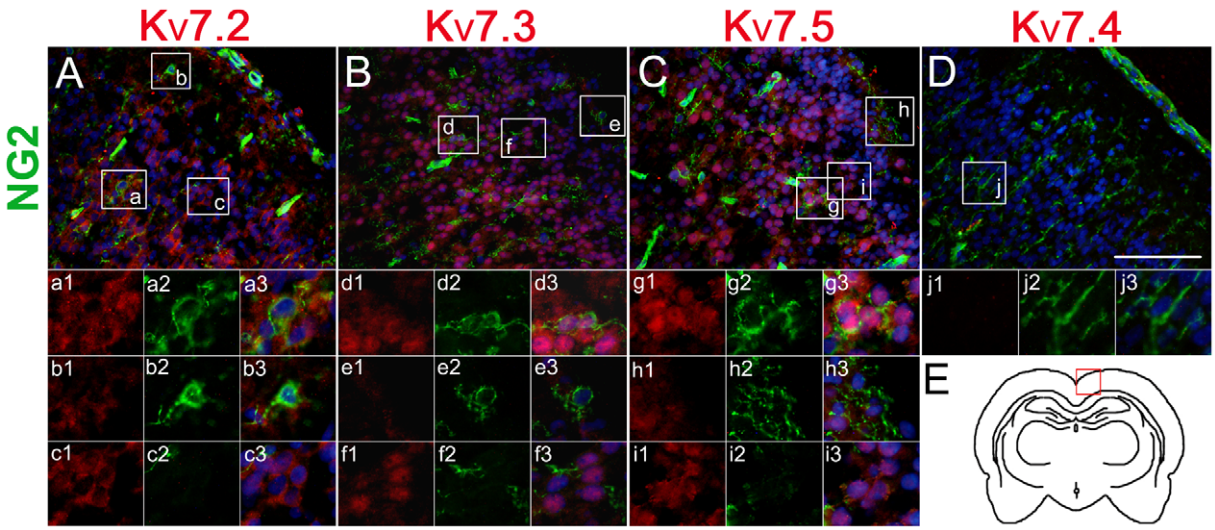

Figure 4. Immunofluorescence localization of K_V7.2-5/KCNQ2-5 on NG2-positive cells (green) of the rat brain slices. (A–C) Co-localization of K_V7.2, 3, 5 and OPCs is displayed in the merged image. Higher magnification of the boxed area in A, B and C was shown in a1–a3; b1–b3;c1–c3;d1–d3;e1–e3;f1–f3;g1–g3;h1–h3 and i1–i3. (D) K_V7.4 was not detected on OPCs. j1–j3: higher magnification of the boxed area in D. The nuclei were stained with Hoechst (blue). (E) Schematic diagram of the brain coronal and the box represented A–D areas. Scar bar = 100 μm.
doi:10.1371/journal.pone.0021792.g004

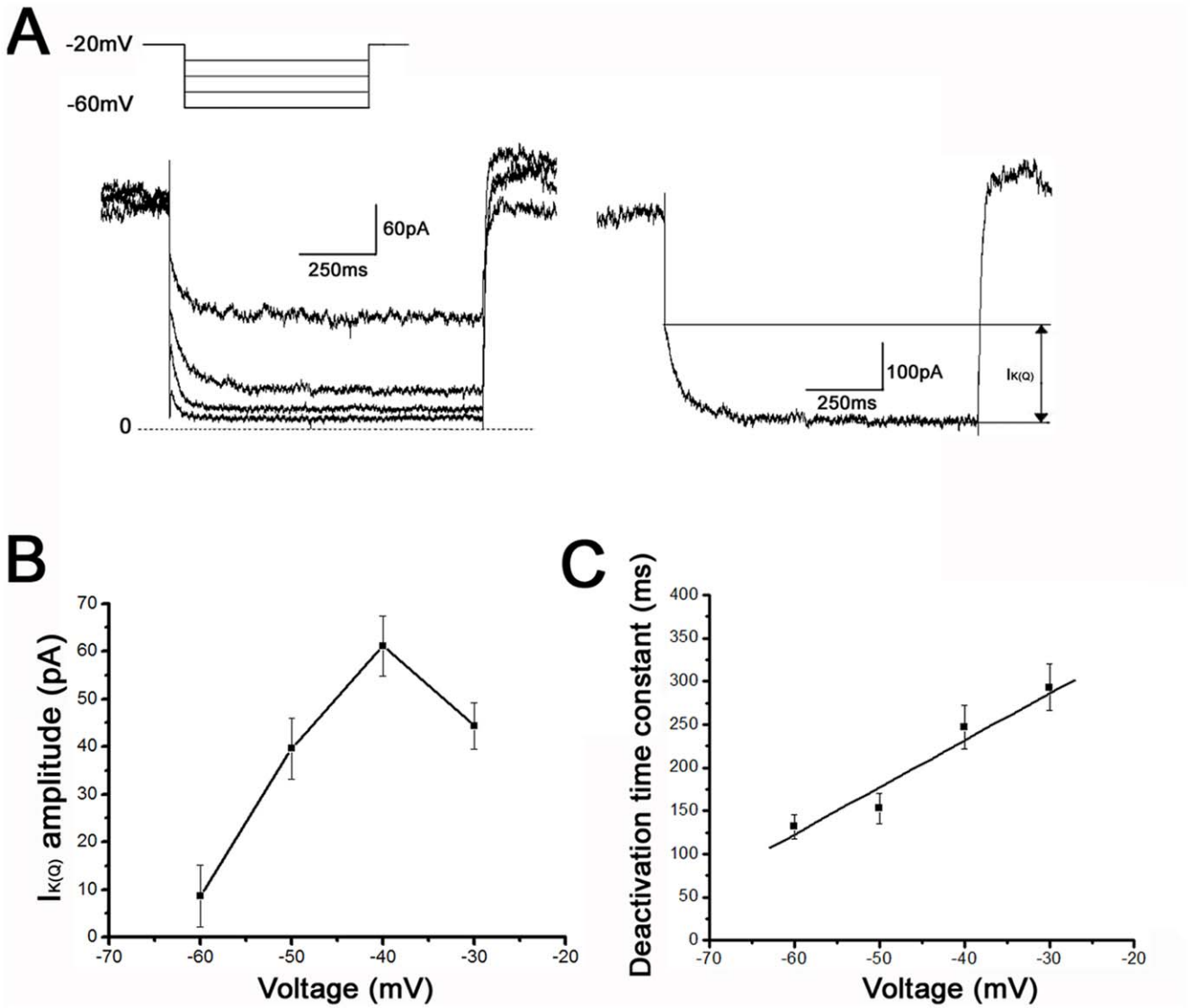

Figure 5. K_V7/KCNQ channel current ($I_{K(Q)}$) in OPCs of rat primary cultures. (A) $I_{K(Q)}$ was measured with whole cell patch clamp recording from OPCs. Left insert: Standard I_M deactivation voltage protocol used to measure $I_{K(Q)}$. Hyperpolarizing voltage steps were given from a holding potential of −20 to −60 mV (in 10 mV decrements). Currents recorded are shown below; the dashed line represents the zero current level. Right: Current recorded in response to the voltage step to −40 mV. $I_{K(Q)}$ was measured as the inward relaxation current caused by deactivation of $I_{K(Q)}$ during the voltage step; i.e., the difference between the instantaneous current at the beginning and the steady-state current at the end of the voltage step (arrows). (B) Current–voltage relationship for $I_{K(Q)}$ (mean data from 17 OPCs) showing that $I_{K(Q)}$ amplitude was voltage dependent and was largest at −40 mV. (C) $I_{K(Q)}$ deactivation time constants were directly related to voltage (mean data from 17 OPCs). Correlation coefficient r = 0.93.
doi:10.1371/journal.pone.0021792.g005

measured the mobility of OPCs cultured in a Boyden chamber. After 8 h incubation with 1 μM, 3 μM or 10 μM XE991 in the lower wells of the chemotaxis chambers, the number of migrated OPCs was significantly increased compared with the control group (Fig.7A, C), suggesting that inhibition of Kv7/KCNQ channels promotes OPCs migration. We also tested the effect of another blocker TEA on OPCs migration. As shown in Figure7 B and D, in the presence of TEA (1 mM, 3 mM or 10 mM) the number of OPCs migrating through the transwell was significantly increased.

Discussion

OLCs express K_V7/KCNQ channels

Neuronal K_V7 channels are constructed from a family of at least four subunits ($K_V7.2$–5) [1,2,5]. These subunits are expressed widely in the brain and prominently localized in several types of neurons [57,58]. Some studies also suggested that a population of glial cells in the white matter expressed the $K_V7.4/5$, but they didn't state clearly the type of glial cells [8,59]. The present study represents the first attempt to identify the K_V7 channel subunits in OLCs. The mRNA of the four genes (KCNQ2-5) was detectable in OPCs. KCNQ3 and KCNQ5 mRNAs were detected strongly, and lesser abundances of mRNAs encoding KCNQ2 and KCNQ4 were observed. KCNQ2-4 mRNAs also existed in IOs with similar expression levels. In MOs, we only find very week sign of KCNQ4 mRNA. These indicated that the transcripts of KCNQ2-5 might be down regulated during the maturation of OLCs. Previous studies found that KCNQ2, 4, 5 genes have alternative splice variants [60-63]. However, the primers used in this study were designed based on regions outside the putative

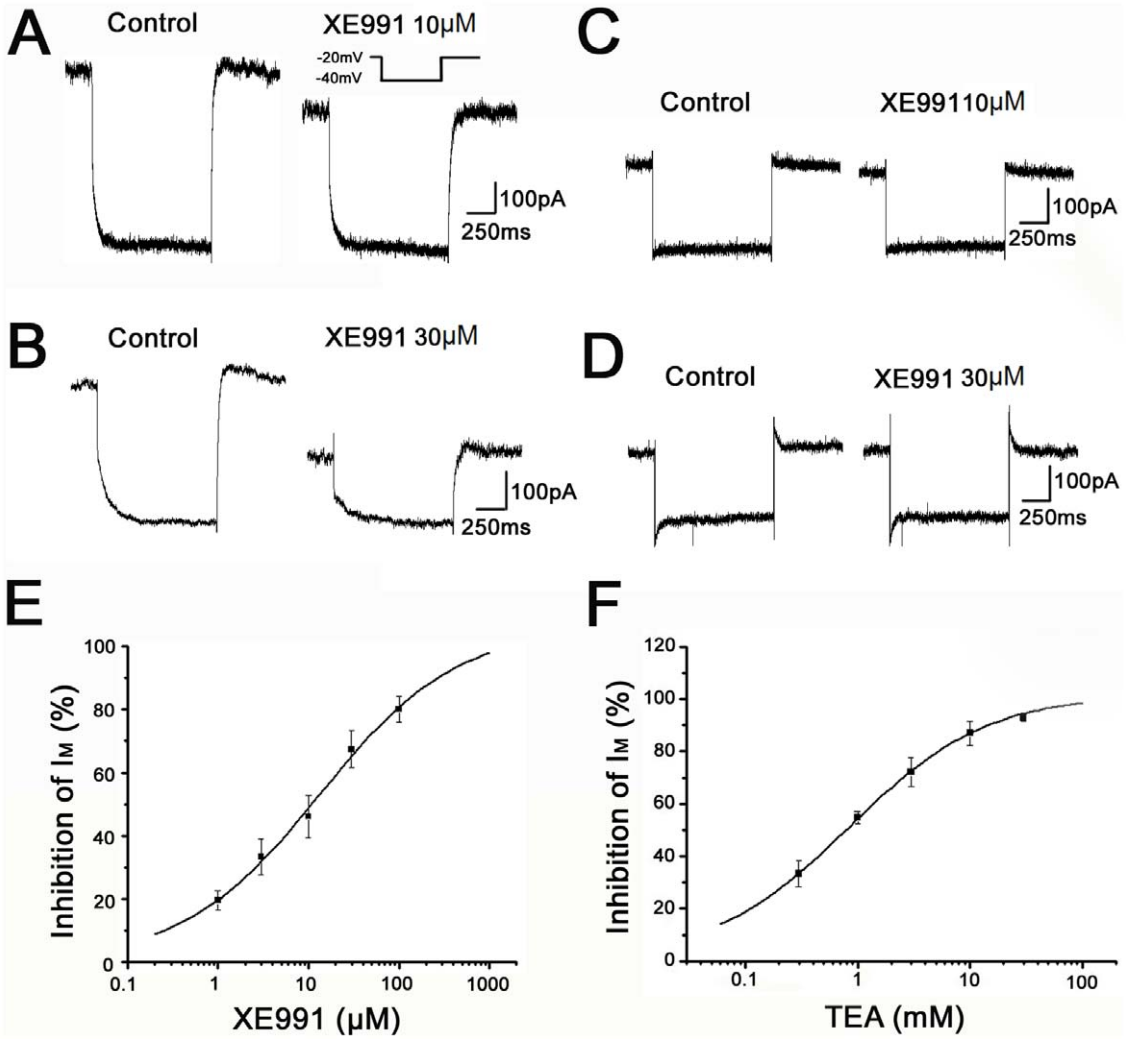

Figure 6. Inhibition of $I_{K(Q)}$ by XE991 and TEA. (A, B) Representative current traces, which were recorded before (Control) and after extracellular application of XE991 (10 μM, 30 μM) in OPCs. (C, D) Representative current traces, which were recorded before (Control) and after extracellular application of XE991 (10 μM, 30 μM) in differentiated oligodendrocytes. Insert: 1-s-long hyperpolarizing voltage step from a holding potential of −20 to −40 mV was given to monitor $I_{K(Q)}$. (E) Concentration–response curve showing the mean percentage inhibition of $I_{K(Q)}$ amplitude as a function of the log XE991 concentration for 54 OPCs. Smooth curve was fit with the Hill equation. IC50 value for XE991 inhibition determined from this pooled log concentration–response curve was 13.3 μM. n = 0.63, R^2 = 0.99. (F) Concentration–response curve showing the mean percentage inhibition of $I_{K(Q)}$ amplitude as a function of the log TEA concentration for 20 OPCs. Smooth curve was fit with the Hill equation. IC50 value for TEA inhibition determined from this pooled log concentration–response curve was 0.84 mM. n = 0.7, R^2 = 0.99.
doi:10.1371/journal.pone.0021792.g006

splice variation position of rat KCNQ2-5 genes. Theoretically, our primers can recognize all of these splice variants but can not distinguish them in OLCs mRNA preparations. We also examed the presence of K_V7.2-5 proteins in cultured OLCs. The signals of four proteins (K_V7.2-5) were weakly detected in differentiated OLCs (IOs and MOs), while they were obviously dyed out in OPCs. In agreement with the immunostaining experiments, the inward deactivation relaxation currents almost did not exist in IOs and MOs. It is likely that the mRNAs for K_V7.2-4, or only K_V7.4 which were detected in IOs and MOs respectively were unable to be translated into enough Kv7 proteins to be detected by immunocytochemistry or electrophysiology method. This developmental regulation may reflect some yet unknown roles played by K_V7 channels in early development of OLCs.

However, previous work on the expression of members of the Kv channel family suggested that the precise topographical distribution of Kv channel subunits in cultured cells may not fully reproduce that obtained in situ [64,65]. Similarly, we detected the immunoreactive signal of K_V7.2, 3 and 5 proteins, but not K_V7.4, in $NG2^+$ OPCs in rat cortex slices. These results agree with the work of Kharkovets et al. [22] that the cortex does not contain K_V7.4 channel transcripts.

The electrophysiological properties of K_V7/KCNQ channels in OPCs

Functional K_V7 channels are composed of four homomeric or heteromeric subunits. The sensitivity to XE991 of these homomeric or heteromeric channel currents differs considerably. Homomeric K_V7.2 channels have an IC_{50} value for XE991 inhibition which is 0.7 μM. The K_V7.2+3 heteromultimer retain the sensitivity of the K_V7.2 homomultimer. However, homomeric K_V7.3 and homomeric K_V7.5 are very insensitive to XE991 with

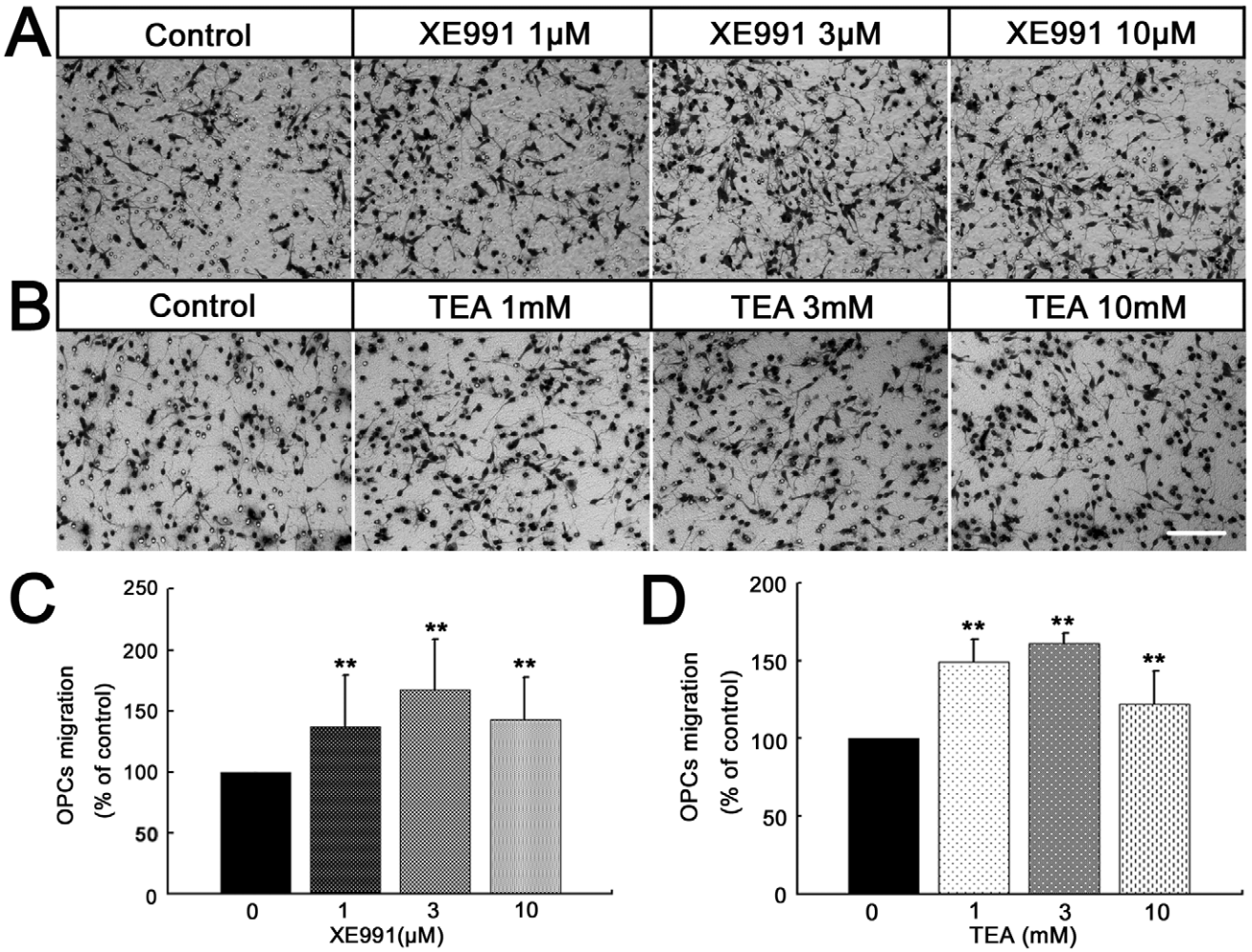

Figure 7. The inhibition of K_V7/KCNQ channels promotes OPCs motility in vitro. (A,B) Photomicrograph of OPCs transmigrated through the filter in the absence or presence of XE991 or TEA. Scar bar = 150 μm. (C, D) Quantitative assessment of migrated cells under different conditions. n(XE991) = 9; n(TEA) = 9. **P<0.01 versus control.
doi:10.1371/journal.pone.0021792.g007

estimated IC_{50} values of <50 μM and 65 μM [2]. In our study, XE991 (10 μM) showed a inhibition of current (by 46.1±6.8%) and high concentration (30 μM) displayed over a half inhibition of $I_{K(Q)}$ (by 67.4±5.6%) in OPCs. The IC50 for XE991 was 13.3 μM.

Different K_V7 channel proteins also have different sensitivities to TEA [55;56;5]. In the present experiments, the $I_{K(Q)}$ relaxations were completely inhibited by TEA with an IC50 of 0.84 mM, which is less than the IC50 for block of artificially expressed homomeric K_V7.4 channels and heteromeric K_V7.2/3 channels currents [5;55], though somewhat higher than the IC50 for block of homomeric K_V7.2 currents. K_V7.2-5 channel proteins were all detected in OPCs, however, their exactly expression level was unknown. The difference of pharmacological sensitivity to XE991 or TEA might due to various expression level and composition of each K_V7 channel subunit in OPCs.

In the present study, the amplitude of $I_{K(Q)}$ in OPCs was found to be voltage dependent, which is similar to I_M measured in sympathetic ganglion, hippocampal and dopamine neurons [3,5,8,66,67]. The maximal $I_{K(Q)}$ amplitude in the OPCs was obtained at −40 mV with the deactivation protocol. The deactivation time constant was voltage dependent in OPCs, becoming shorter at more hyperpolarized membrane potentials, as has been observed for native I_M currents in neuronal cell types [3,5,10,67]. The time course of $I_{K(Q)}$ deactivation in OPCs was well fitted with a single exponential function and the value of the deactivation time constant was 152.85 ms at −50 mV. The deactivation time constant in OPCs seems to be closest to the fast component of the deactivation time constant in sympathetic neurons, which was reported to be 145 ms at −50 mV [5]. Native I_M currents in neurons have a biphasic (double-exponential) time course [5,8,10]. The absence of this slow component of deactivation in our experiments could be attributable to a difference in the types of K_V7 channels underlying $I_{K(Q)}$ in OPCs.

Function of K_V7/KCNQ in OPCs

During development, OLCs express all six members of the delayed rectifier Shaker family K^+ channels, Kv1.1–Kv1.6 [40–45], inwardly rectifying K^+ (K_{ir}) channels Kir2.1, Kir1.1 and Kir4.1 [46,47] and Kv3.1 [29]. In our experiments, we found that K_V7 channels were expressed in OLCs, and downregulated in IOs and MOs. This developmental regulation may reflect some yet unknown roles played by K_V7 channels in early OLCs development.

Migration of OPCs from proliferation zones to their final position is an essential step in the development of the nervous system [26,68,69], yet the physiological mechanisms of OPCs migration are still largely unknown. The idea that the K^+ channels may be linked to cell migration is supported by several studies [36–39]. Importantly, $K_V7.1$ potassium channels have been implicated recently in the regulation of migration and invasiveness of stem-like cell types [35]. Our results support the concept that K_V7 channels are important for the regulation of OPCs migration in vitro. In our migration assay, the motility of the OPCs was promoted by the inhibition of K_V7 channels. In fact, in neurons, K_V7 channels can be inhibited by many endogenous factors. For example, stimulation of a variety of Gq/11-coupled neurotransmitter receptors, local changes in PIP2 concentration [70–72] and calmodulin [73], etc. In dissociated rat superior cervical sympathetic neurons, purinergic P2Y receptors can couple to G protein thereby modulating K_V7 channel [74]. Agresti et al. [32] found that activation of P2Y1 receptors by ATP can promote OPCs migration. It is likely that ATP released following neuronal activity, astrocyte Ca^{2+} waves or cell lysis [75,76] might inhibit K_V7 channels though P2Y1, and consequently promote the OPCs migration.

Materials and Methods

Oligodendrocyte lineage cell cultures

The animal experiments were carried out in adherence with the National Institutes of Health Guidelines on the Use of laboratory Animals and were approved by Second Military Medical University Committee on Animal Care (permission №: SCXK-HU-2007-0003). OLCs were prepared as previously described [77,78] with slight modification. Briefly, cortex was dissected from postnatal day 1–2 Sprague Dawley rats, dissociated in Hanks balanced salt solution containing 0.125% trypsin (GIBCO, Canada) for 20 min, 37°C, suspended in DMEM containing 10% fetal bovine serum (FBS, BIOSOURCE, Brazil), and plated in plastic T75 flasks. After about 10 days in culture, OPCs growing on top of a confluent monolayer of astrocytes were detached by overnight shaking. Contaminating microglial cells were further eliminated by plating this fraction on plastic culture dishes for 1 hr. The OPCs, which do not attach well to plastic, were collected by gently washing the dishes, replated (3×10^4 cells/cm^2) onto poly-L-lysine-precoated plates (0.1 mg/ml) and cultured in DMEM containing 10% FBS medium. After 2 hr, DMEM supplemented with 30% B104 neuroblastoma conditioned medium, 1% B27 (GIBCO, Canada) and 1% N2 (GIBCO, Canada) was added to the culture medium. Immature oligodendrocytes (IOs) were produced by substitution of DMEM, 30% B104, 1% B27 and 1% N2 with Neurobasal medium (GIBCO, Canada) containing 1% B27, 1% N2, T3 (40 ng/ml) and biotin (10 ng/ml) for 2 days, and mature oligodendrocytes (MOs) by substitution with that medium for 4 days.

RT-PCR and Quantitative PCR

Total RNA was extracted from adult rat forebrain or cultured OLCs using TRIZOL Reagent (Invitrogen Corporation, Carlsbad, CA), followed by the treatment with DNase I RNA-free (Fermentas, USA). Synthesis of cDNA was carried out with the Superscript First-Strand Synthesis System for RT-PCR (Invitrogen Corporation, Carlsbad, CA). The RNA from OLCs without reverse transcription was performed PCR procedure directly as negative control, while the RNA from adult rat forebrain was as positive control. The PCR temperature profile was 94°C for 3 min, followed by 40 cycles of 94°C for 30 s, 60°C for 30 s, and 72°C for 1 min, 72°C 5 min. All primers are listed in Table1.

Table 1. Primers for PCR.

Gene	Accession no.	Primer(5′–3′)	Product size(bp)
KCNQ2	NM133322	F: GGTGCTGATTGCCTCCATT R: CTCCTTGCTGTGAGCGTAGAC	172 bp
KCNQ3	NM031597	F: CCCCTATTCGGACCACATC R: GCTGAAGCCACTTGGAGACC	121 bp
KCNQ4	XM233477	F: GACGATTACACTGACGACCATT R: GCAGGGCAAAGAAGGAGAT	110 bp
KCNQ5	XM001071249	F: GCTGGGCTCCGTGGTTTA R: TCTGGCGGTGCTGTTCCT	320 bp
GAPDH	NM017008	F:TCTGACATGCCGCCTGGAGAAA-CCTGC R:CACCACCCTGTTGCTGTAGCCAT-ATTCATTGTC	243 bp

Specifies forward (F) and reverse (R) primers used for RT-PCR of rat KCNQ channel subunits and GAPDH.
doi:10.1371/journal.pone.0021792.t001

Immunocytochemistry and immunohistochemistry

For immunocytochemical analysis, OLCs on coverslips were washed with phosphate buffered saline (PBS) and fixed with 4% paraformaldehyde (PFA) in PBS for 20 min, followed by permeabilization with 0.3% Triton X-100 in 0.1 M PBS for 10 minutes. After blocking the non-specific binding with 10% normal goat serum or 1% BSA in 0.1 M PBS, cells were incubated with primary antibodies against A2B5 (Chemicon, USA), GFAP (Sigma, USA), NG2 (Chemicon, USA), O4 (Sigma, USA), MBP (Chemicon,USA), $K_V7.2$, 3 (Chemicon, USA) , $K_V7.4$ (Santa Cruz, USA) and $K_V7.5$ (Millipore, USA) at 4°C overnight. Cells were then washed and incubated with fluorescence-conjugated secondary antibodies (Jackson ImmunoResearch Laboratories, Inc.) for 6 hours at room temperature and examined by fluorescence microscopy (Nikon, Japan). For immunohistochemical analysis, animals were deeply anaesthetized with 2% pentobarbital sodium and perfused transcardially with 4% PFA in 0.1 M PBS, pH 7.4. The brain were subsequently dissected from each animal and post-fixed in the perfusing solution overnight at 4°C. Then, the tissues were cryoprotected in 20% sucrose in PBS for 24–48 h at 4°C. Cryostat sections (10 μm) were cut and mounted onto gelatin-subbed slides and stored at −20°C. For immunostaining, the protocol performed was similar to immunocytochemical analysis.

Electrophysiological recordings

Current recordings were performed in the whole cell configuration of the patch-clamp technique using MultiClamp700A amplifier (Axon, USA). Date were stored in a PC, and analyzed by pClamp8.02 software (Axon Instruments, Sunnyvale, CA, USA). The patch pipettes (6~8 MΩ), pulled using a Narishige puller (PP-83, Japan) and polished using a MF200 Microforge (WPI, USA), were filled with solution containing 140 mM KCl, 4 mM $MgCl_2$, 0.1 mM EGTA, 4 mMATP·2Na, 0.5 mM Na_3·GTP, and 10 mM HEPES (pH 7.4 with KOH). The superfusate solution used to measure $I_{K(Q)}$ contained 150 mM NaCl, 5 mM KCl, 1 mM $MgCl_2$, 2 mM$CaCl_2$, 10 mM HEPES, and 10 mM Glucose (pH 7.4 with NaOH). All experiments were done in room temperature. Drugs were applied through OctaFlow System (ALA, USA) to the cell under recording. XE991 (Sigma, USA) and TEA (Sigma, USA) was dissolved in water to store at −20°C, and diluted part per thousand using superfusate solution.

Hyperpolarizing voltage steps (1 s duration) were given from a holding potential of −20 to −60 mV (in 10-mV increments).

Graphing and curve fitting of data were performed with Origin 7 software (OriginLab, Northampton, MA). The inward relaxation current, which was attributed to deactivation of $I_{K(Q)}$, was fitted by a single exponential function $I(t)=Ae^{-\frac{t}{\tau}}$. Where A is amplitude obtained from the beginning of the fit and τ is the decay time constant.

Concentration-response curves for XE991 and TEA were constructed by plotting percentage inhibition of $I_{K(Q)}$ as a function of drug concentration plotted on a log scale. Smooth curves were fit to these data with the Hill equation $y=y_{max}x^n/(k^n+x^n)$.

Where x is the concentration, y is the percentage inhibition, and y_{max} is the maximal value of y (at saturation); in the fitting procedure y_{max} was constrained not to exceed 100%. The term k is the IC50 (the concentration giving half-maximal inhibition) and n (Hill slope) is the power term related to the slope of the curve.

Boyden chamber migration assay

To measure the motility of OPCs, Boyden chamber migration assay was performed as previously described [79]. In brief, the polyethylene terephthalate filter membranes were coated with poly-L-lysine. The purified OPCs were seeded onto the upper chamber at a density of 2×10^5 cells in 200 µl of culture medium containing 10% FBS per well, and 600 uL DMEM containing 10% FBS were added to lower chamber. When OPCs were adherent (about 40 min later), the DMEM medium containing 10% FBS in the upper and lower chamber was replaced with serum-free DMEM supplemented with 30% B104 neuroblastoma conditioned medium, 1%B27, and 1%N2. XE991 or TEA was added to the lower chamber. After incubation for 8 h at 37°C, non-migratory cells on the upper membrane surface were removed with a cotton swab, and migratory cells invading to the underside surface of the membrane were fixed with 4% paraformaldehyde and stained with Coomassie Brilliant Blue. For quantitative assessment, the number of stained cells was counted under microscopy at 12 fields per filter in three independent experiments.

Statistical analysis

Data from at least three independent experiments were all presented as means ± SEM. Statistical significance was evaluated with paired Student's t-test. Differences were considered significant at $p<0.05$.

Acknowledgments

We thank Professor Hai-Lin Zhang in Hebei Medical University for his helpful suggestions and comments in electrophysiological work.

Author Contributions

Conceived and designed the experiments: WW X-FG CH. Performed the experiments: WW X-FG LX Z-HX. Analyzed the data: WW X-FG. Contributed reagents/materials/analysis tools: WW X-FG. Wrote the paper: WW X-FG CH.

References

1. Jentsch TJ (2000) Neuronal KCNQ potassium channels: physiology and role in disease. Nat Rev Neurosci 1: 21–30.
2. Robbins J (2001) KCNQ potassium channels: physiology, pathophysiology, and pharmacology. Pharmacol Ther 90: 1–19.
3. Brown DA, Adams PR (1980) Muscarinic suppression of a novel voltage-sensitive K^+ current in a vertebrate neurone. Nature 283: 673–676.
4. Brown DA (1988) M currents. Ion Channels 1: 55–94.
5. Wang HS, Pan Z, Shi W, Brown BS, Wymore RS, et al. (1998) KCNQ2 and KCNQ3 potassium channel subunits: molecular correlates of the M-channel. Science 282: 1890–1893.
6. Hadley JK, Passmore GM, Tatulian L, Al-Qatari M, Ye F, et al. (2003) Stoichiometry of expressed KCNQ2/KCNQ3 channels and subunit composition of native ganglionic M-channels deduced from block by tetraethyl ammonium (TEA). J Neurosci 23: 5012–5019.
7. Schwarz JR, Glassmeier G, Cooper E, Kao T, Nodera H, et al. (2006) KCNQ channels mediate IKs, a slow K^+ current regulating excitability in the node of Ranvier. J Physiol 573: 17–34.
8. Shah MM, Mistry M, Marsh SJ, Brown DA, Delmas P (2002) Molecular correlates of the M-current in cultured rat hippocampal neurons. J Physiol 54: 29–37.
9. Hansen HH, Waroux O, Seutin V, Jentsch TJ, Aznar S, et al. (2008) Kv7 channels: interaction with dopaminergic and serotonergic neurotransmission in the CNS. J Physiol 586: 1823–1832.
10. Passmore GM, Selyanko AA, Mistry M, Al-Qatari M, Marsh SJ, et al. (2003) KCNQ/M currents in sensory neurons: significance for pain therapy. J Neurosci 23: 7227–7236.
11. Zaika O, Lara LS, Gamper N, Hilgemann DW, Jaffe DB, et al. (2006) Angiotensin-II regulates neuronal excitability via PIP2-dependent modulation of Kv7 (M-type) potassium channels. J Physiol 575: 49–67.
12. Lang PM, Fleckenstein J, Passmore GM, Brown DA, Grafe P (2008) Retigabine reduces the excitability of unmyelinated peripheral human axons. Neuropharmacology 54: 1271–1278.
13. Wladyka CL, Feng B, Glazebrook PA, Schild JH, Kunze DL (2008) The KCNQ/M-current modulates arterial baroreceptor function at the sensory terminal in rats. J Physiol 586: 795–802.
14. Yue C, Yaari Y (2004) KCNQ/M channels control spike afterdepolarization and burst generation in hippocampal neurons. J Neurosci 24: 4614–4624.
15. Liu B, Linley JE, Du X, Zhang X, Ooi L, et al. (2010) The acute nociceptive signals induced by bradykinin in rat sensory neurons are mediated by inhibition of M-type K^+ channels and activation of $Ca2^+$-activated Cl^- channels. J Clin Invest 120: 1240–1252.
16. Aiken SP, Lampe BJ, Murphy PA, Brown BS (1995) Reduction of spike frequency adaptation and blockade of M-current in rat CA1 pyramidal neurones by linopirdine (DuP 996), a neurotransmitter release enhancer. Br J Pharmacol 115: 1163–1168.
17. Peters HC, Hu H, Pongs O, Storm JF, Isbrandt D (2005) Conditional transgenic suppression of M channels in mouse brain reveals functions in neuronal excitability, resonance and behavior. Nat Neurosci 8: 51–60.
18. Biervert C, Schroeder BC, Kubisch C, Berkovic SF, Propping P, et al. (1998) A potassium channel mutation in neonatal human epilepsy. Science 279: 403–406.
19. Schroeder BC, Hechenberger M, Weinreich F, Kubisch C, Jentsch TJ (2000) KCNQ5, a novel potassium channel broadly expressed in brain, mediates M-type currents. J Biological Chemistry 275: 24089–24095.
20. Kananura C, Biervert C, Hechenberger M, Engels H, Steinlein OK (2000) The new voltage gated potassium channel KCNQ5 and neonatal convulsions. Neuroreport 11: 2063–2067.
21. Kubisch C, Schroeder BC, Friedrich T, Lütjohann B, El-Amraoui A, et al. (1999) KCNQ4, a novel potassium channel expressed in sensory outer hair cells, is mutated in dominant deafness. Cell 96: 437–446.
22. Kharkovets T, Hardelin JP, Safieddine S, Schweizer M, El-Amraoui A, et al. (2000) KCNQ4, a K^+ channel mutated in a form of dominant deafness, is expressed in the inner ear and the central auditory pathway. Proc Natl Acad Sci U S A 97: 4333–4338.
23. Kharkovets T, Dedek K, Maier H, Schweizer M, Khimich D, et al. (2006) Mice with altered KCNQ4 K^+ channels implicate sensory outer hair cells in human progressive deafness. EMBO J 25: 642–652.
24. Richardson WD, Kessaris N, Pringle N (2006) Oligodendrocyte wars. Nat Rev Neurosci 7: 11–18.
25. Bradl M, Lassmann H (2010) Oligodendrocytes: biology and pathology. Acta Neuropathol 119: 37–53.
26. Kessaris N, Fogarty M, Iannarelli P, Grist M, Wegner M, et al. (2006) Competing waves of oligodendrocytes in the forebrain and postnatal elimination of an embryonic lineage. Nat Neurosci 9: 173–179.
27. McTigue, DM, Tripathi, RB (2008) The life, death, and replacement of oligodendrocytes in the adult CNS. J Neurochem 107: 1–19.
28. Blakemore WF, Keirstead HS (1999) The origin of remyelinating cells in the central nervous system. J Neuroimmunol 98: 69–76.
29. Tiwari-Woodruff S, Beltran-Parrazal L, Charles A, Keck T, Vu T, et al. (2006) K^+ channel $K_V3.1$ associates with OSP/claudin-11 and regulates oligodendrocyte development. Am J Physiol Cell Physiol 291: C687–698.
30. Paez PM, Fulton DJ, Spreuer V, Handley V, Campagnoni CW, et al. (2009) Golli myelin basic proteins regulate oligodendroglial progenitor cell migration through voltage-gated Ca^{2+} influx. J Neurosci 29: 6663–6676.
31. Paez PM, Fulton DJ, Spreur V, Handley V, Campagnoni AT (2010) Multiple kinase pathways regulate voltage-dependent Ca^{2+} influx and migration in oligodendrocyte precursor cells. J Neurosci 30: 6422–6433.
32. Agresti C, Meomartini ME, Amadio S, Ambrosini E, Volonté C, et al. (2005) ATP regulates oligodendrocyte progenitor migration, proliferation, and differentiation: involvement of metabotropic P2 receptors. Brain Res Brain Res Rev 482: 157–65.

33. Luyt K, Slade TP, Dorward JJ, Durant CF, Wu Y, et al. (2007) Developing oligodendrocytes express functional GABA (B) receptors that stimulate cell proliferation and migration. J Neurochem 1003: 822–840.
34. Gudz TI, Komuro H, Macklin WB (2006) Glutamate stimulates oligodendrocyte progenitor migration mediated via an alphav integrin/myelin proteolipid protein complex. J Neurosci 269: 2458–2466.
35. Morokuma J, Blackiston D, Levin M (2008) KCNQ1 and KCNE1 K^+ channel components are involved in early left-right patterning in Xenopus laevis embryos. Cell Physiol Biochem 21: 357–372.
36. Rao JN, Platoshyn O, Li L, Guo X, Golovina VA, et al. (2002) Activation of K^+ channels and increased migration of differentiated intestinal epithelial cells after wounding. Am J Physiol Cell Physiol 282: 885–898.
37. Toral C, Mendoza-Garrido ME, Azorín E, Hernández-Gallegos E, Gomora JC, et al. (2007) Effect of extracellular matrix on adhesion, viability, actin cytoskeleton and K^+ currents of cells expressing human ether à go-go channels. Life Sci 81: 255–265.
38. Lastraioli E, Guasti L, Crociani O, Polvani S, Hofmann G, et al. (2004) herg1 gene and HERG1 protein are overexpressed in colorectal cancers and regulate cell invasion of tumor cells. Cancer Res 64: 606–611.
39. Matheu MP, Beeton C, Garcia A, Chi V, Rangaraju S, et al. (2008) Imaging of effector memory T cells during a delayed-type hypersensitivity reaction and suppression by Kv1.3 channel block. Immunity 29: 602–614.
40. Bacia A, Wollmann R, Soliven B (2004) K^+ channel blockade impairs remyelination in the cuprizone model. Glia 48: 156–165.
41. Chittajallu R, Chen Y, Wang H, Yuan X, Ghiani CA, et al. (2002) Regulation of Kv1 subunit expression in oligodendrocyte progenitor cells and their role in G1/S phase progression of the cell cycle. Proc Natl Acad Sci U S A 99: 2350–2355.
42. Gallo V, Zhou JM, McBain CJ, Wright P, Knutson PL, et al. (1996) Oligodendrocyte progenitor cell proliferation and lineage progression are regulated by glutamate receptor-mediated K^+ channel block. J Neurosci 16: 2659–2670.
43. Knutson P, Ghiani CA, Zhou JM, Gallo V, McBain CJ (1997) K^+ channel expression and cell proliferation are regulated by intracellular sodium and membrane depolarization in oligodendrocyte progenitor cells. J Neurosci 17: 2669–2682.
44. Shrager P, Novakovic SD (1995) Control of myelination, axonal growth, and synapse formation in spinal cord explants by ion channels and electrical activity. Brain Res Dev Brain Res 88: 68–78.
45. Attali B, Wang N, Kolot A, Sobko A, Cherepanova V, et al. (1997) Characterization of delayed rectifier Kv channels in oligodendrocytes and progenitor cells. J Neurosci 17: 8234–8245.
46. Karschin A, Wischmeyer E (1995) Identification of G protein-regulated inwardly rectifying K^+ channels in rat brain oligodendrocytes. Neurosci Lett 183: 135–138.
47. Neusch C, Rozengurt N, Jacobs RE, Lester HA, Kofuji P (2001) Kir4.1 potassium channel subunit is crucial for oligodendrocyte development and in vivo myelination. J Neurosci 21: 5429–5438.
48. Dubois-Dalcq M (1987) Characterization of a slowly proliferative cell along the oligodendrocyte differentiation pathway. EMBO J 6: 2587–2595.
49. Gard AL, Pfeiffer SE (1989) Oligodendrocyte progenitors isolated directly from developing telencephalon at a specific phenotypic stage: myelinogenic potential in a defined environment. Dev Biol 106: 119–132.
50. Adams PR, Brown DA (1982) Synaptic inhibition of the M-current: slow excitatory post-synaptic potential mechanism in bullfrog sympathetic neurones. J Physiol (Lond) 332: 263–272.
51. Nisenbaum ES, Wilson CJ, Foehring RC, Surmeier DJ (1996) Isolation and characterization of a persistent potassium current in neostriatal neurons. J Neurophysiol 76: 1180–1194.
52. Tkatch T, Baranauskas G, Surmeier DJ (2000) Kv4.2 mRNA abundance and A-type K^+ current amplitude are linearly related in basal ganglia and basal forebrain neurons. J Neurosci 20: 579–588.
53. Shen W, Hernandez-Lopez S, Tkatch T, Held JE, Surmeier DJ (2004) Kv1.2-containing K^+ channels regulate subthreshold excitability of striatal medium spiny neurons. J Neurophysiol 91: 1337–1349.
54. Wladyka CL, Kunze DL (2006) KCNQ/M-currents contribute to the resting membrane potential in rat visceral sensory neurons. J Physiol 5750: 175–189.
55. Hadley JK, Noda M, Selyanko AA, Wood IC, Abogadie FC, et al. (2000) Differential tetraethylammonium sensitivity of KCNQ1-4 potassium channels. Br J Pharmacol 129: 413–415.
56. Shapiro MS, Roche JP, Kaftan EJ, Cruzblanca H, Mackie K, et al. (2000) Reconstitution of muscarinic modulation of the KCNQ2/KCNQ3 K^+ channels that underlie the neuronal M current. J Neurosci 20: 1710–1721.
57. Cooper EC, Harrington E, Jan YN, Jan LY (2001) M channel KCNQ2 subunits are localized to key sites for control of neuronal network oscillations and synchronization in mouse brain. J Neurosci 21: 9529–9540.
58. Saganich MJ, Machado E, Rudy B (2001) Differential expression of genes encoding subthreshold-operating voltage-gated K^+ channels in brain. J Neurosci 21: 4609–4624.
59. Yus-Nájera E, Muñoz A, Salvador N, Jensen BS, Rasmussen HB, et al. (2003) Localization of KCNQ5 in the normal and epileptic human temporal neocortex and hippocampal formation. Neuroscience 120: 353–364.
60. Tinel N, Lauritzen I, Chouabe C, Lazdunski M, Borsotto M (1998) The KCNQ2 potassium channel: splice variants, functional and developmental expression. Brain localization and comparison with Kcnq3. FEBS Lett 438: 171–176.
61. Jeffrey SS, Claudia AI, Pauline D, Edward PC, Jayashree A (2001) Differential Expression of KCNQ2 Splice Variants: Implications to M Current Function during Neuronal Development. J Neurosci 21: 1096–1103.
62. BjÖrn CS, Mirko H, Frank W, Christian K, Thomas JJ (2000) KCNQ5, a Novel Potassium Channel Broadly Expressed in Brain, Mediates M-type Currents. J Biological chemistry 275: 24089–24095.
63. Kirk WB, Sonia MRS, Ken AM, Liping N, Feng F, et al. (2005) Differential Expression of KCNQ4 in Inner Hair Cells and Sensory Neurons Is the Basis of Progressive High-Frequency Hearing Loss. J Neurosci 2540: 9285–9293.
64. Maletic-Savatic M, Lenn NJ, Trimmer JS (1998) Differential spatiotemporal expression of K^+ channel polypeptides in rat hippocampal neurons developing in situ and in vitro. J Neurosci 15: 3840–3851.
65. Grosse G, Draguhn A, Höhne L, Tapp R, Veh RW, et al. (2000) Expression of Kv1 potassium channels in mouse hippocampal primary cultures: development and activity-dependent regulation. J Neurosci 20: 1869–1882.
66. Schweitzer P (2000) Cannabinoids decrease the K^+ M-current in hippocampal CA1 neurons. J Neurosci 20: 51–58.
67. Koyama S, Appel SB (2006) Characterization of M-current in ventral tegmental area dopamine neurons. J Neurophysiol 96: 535–543.
68. Ivanova A, Nakahira E, Kagawa T, Oba A, Wada T, et al. (2003) Evidence for a second wave of oligodendrogenesis in the postnatal cerebral cortex of the mouse. J Neurosci Res 73: 581–592.
69. Baumann N, Pham-Dinh D (2001) Biology of oligodendrocyte and myelin in the mammalian central nervous system. Physiol Rev 81: 871–927.
70. Zhang H, Craciun LC, Mirshahi T, Rohács T, Lopes CM, et al. (2003) PIP(2) activates KCNQ channels, and its hydrolysis underlies receptor-mediated inhibition of M currents. Neuron 37: 963–975.
71. Delmas P, Brown DA (2005) Pathways modulating neural KCNQ/M (Kv7) potassium channels. Nat Rev Neurosci 6: 850–862.
72. Brown DA, Passmore GM (2009) Neural KCNQ (Kv7) channels. Br J Pharmacol 156: 1185–1195.
73. Gamper N, Shapiro MS (2003) Calmodulin mediates $Ca2^+$-dependent modulation of M-type K^+ channels. J Gen Physiol 122: 17–31.
74. Brown DA, Filippov AK, Barnard EA (2000) Inhibition of potassium and calcium currents in neurones by molecularly-defined P2Y receptors. J Auton Nerv Syst 81: 31–36.
75. Pankratov Y, Lalo U, Verkhratsky A, North RA (2006) Vesicular release of ATP at central synapses. Pflugers Arch 452: 589–597.
76. Schipke CG, Boucsein C, Ohlemeyer C, Kirchhoff F, Kettenmann H (2002) Astrocyte Ca^{2+} waves trigger responses in microglial cells in brain slices. FASEB J 16: 255–257.
77. Armstrong RC, Harvath L, Dubois-Dalcq M (1990) Type 1 astrocytes and oligodendrocytes-type 2 astrocytes glial progenitors migrate toward distinct molecules. J Neurosci Res 27: 400–407.
78. McKinnon RD, Matsui T, Dubois-Dalcq M, Aaronson SA (1990) FGF modulates the PDGF-driven pathway of oligodendrocyte development. Neuron 5: 603–614.
79. Cao L, Su ZD, Zhou Q, Lv BL, Liu XJ, et al. (2006) Glial cell line-derived neurotrophic factor promotes olfactory ensheathing cells migration. Glia 54: 536–544.